**Highlights (for review)

Highlights

>Critical thresholds of soil water status, identifying olive water stress, were determined.

>Experiments evidenced a threshold of soil matric potential h ≈-40 m below which actual transpiration starts to decrease.

> For soil matric potentials h>-40 m actual transpiration is constant and approximately 2.0 mmd^{-1}.

> A convex shape better represents, for olive trees, the initial phase of the reduction transpiration process

> For olive trees, reductions of actual transpiration become severe only for extreme water stress

*Manuscript
Click here to download Manuscript: MANUSCRIPT.pdf
Click here to view linked References

Modelling eco-physiological response of table olive trees (*Olea europaea L.*) to soil water deficit conditions

Rallo G.[1], Agnese C.[2], Provenzano G.[3]

[1]PhD, Junior Investigator. Dipartimento dei Sistemi Agro-Ambientali (SAgA), Università degli Studi, Viale delle Scienze 12, Palermo (corresponding author). email: rallo.giovanni@gmail.com

[2]Full Professor, retired. Dipartimento dei Sistemi Agro-Ambientali (SAgA), Università degli Studi, Viale delle Scienze 12, Palermo.

[3]PhD, Associate Professor. Dipartimento dei Sistemi Agro-Ambientali (SAgA), Università degli Studi, Viale delle Scienze 12, Palermo.

Abstract

Crop response to water stress is very important to predict transpiration reductions under limited soil water conditions and it can be evaluated according to global stress indicators like relative transpiration or xylematic water potential. Assessing empirical functions able to describe the plant response to water stress, on the basis of parameters depending on the soil or crop water status, is crucial for a rational scheduling of irrigation.

In order to assess whatever water stress model, it is necessary to estimate critical thresholds of soil water status, below which plant transpiration starts to decrease.

The main objective of the work is to identify the shape and to determine the parameters of table olive orchards water stress function, assessed according to relative transpiration or leaf/stem water potential.

The study area, located in the South-Western coast of Sicily (Italy), where table olive orchards are the principal crop, is characterized by typical Mediterranean semi-arid climate. Experiments were carried out during irrigation seasons 2008 and 2009 in a farm mainly cultivated with olive grove (*Olea europaea*, var. Nocellara del Belice) with plants of about 15 years old, spaced 8 m x 5 m. Irrigation water was supplied by means of a drip system, with irrigation timing and doses scheduled according to the ordinary management of the area.

Meteorological data were collected by a weather station located nearby the experimental lay-out.

The collected data allowed to assess different water stress functions describing the crop eco-physiological field response to soil water status.

Thresholds of soil water content and matric potential below which actual transpiration decreases with soil water content were obtained. For values of soil water contents higher than the critical threshold, actual transpiration resulted almost constant. A similar behavior was observed when the xylematic leaf/stem water potentials were used to quantify the crop water stress. Investigation also showed that the non-linear models better reproduced the initial phase of the transpiration reduction process; for the examined crop, in fact, convex shape models typical of xerophytes, better reproduced the reductions of actual transpiration under the soil water deficit conditions recognized in the field.

Keywords: Water stress functions, Sap flow, Leaf/Stem water potentials.

Introduction

Table Olive varieties play an important role in the agricultural and processing sectors of the Mediterranean countries. In the past, olive orchards were mostly rain fed, due to their resilience to water scarcity. The practice of irrigation is relatively new; it has been introduced in order to increase significantly the crop productions and to improve the yield quality (Patumi et al., 2002; D'Andria et al., 2004).

Several researches have been focusing on the optimization of irrigation for olive trees (Rosseaux et al., 2009; Fernández et al., 2006; Tognetti et al., 2004) and it has been recognized how, maintaining olive trees under slight or moderate water stress at specific phenological stages, can contribute to optimize the crop productivity and water use efficiency (Patumi et al., 1999; Berenguer et al., 2006; Caruso et al., 2011).

Impact of water stress as well as its feasible duration and intensity, in fact, depends on crop phenological stages in which the stress occurs. Defining irrigation doses and timing under slight or moderate water stress levels, requires to monitor the water status in the soil-crop system and to identify affordable indicators, able to provide suggestions for irrigation scheduling aimed to achieve desired outcomes.

Soil-Plant-Atmosphere (SPA) water exchanges can be assessed by direct measurements of soil water content, plant water status and environmental variables that, linked to mathematical models, can allow to identify the complex interactions across the SPA continuum (Minacapilli et al., 2008; Cammalleri et al., 2010 a).

Estimation of actual evapotranspiration can be obtained using soil water balance and/or energy balance approaches (Minacapilli et al., 2009; Cammalleri et al., 2010 b; Rallo et al., 2012). With these approaches it is possible to consider the existence of plant water stress through the reductions of root water uptake and/or flux transpiration, both representing the natural response of plant to soil water deficit. Such reductions are usually schematized by means of a linear function.

Two approaches have been proposed to evaluate the crop transpiration: the "microscopic approach" considering the water movement toward and into individual roots (Personne et al., 2003) and the "macroscopic approach" in which a sink-term represents the water extraction by plant roots (Skaggs et al., 2006).

Because the first approach requires a detailed knowledge of the root characteristics, quite difficult to determine, the latter is generally preferred in practical applications.

The macroscopic approach consider global stress indicators (relative transpiration, xylematic water potential, etc), without regarding the flow patterns toward individual roots, and avoiding the need of analyzing the potential gradients distribution in the soil-roots interface. Using this approach it is possible to assess empirical functions able to describe the plant response to water stress, on the basis of parameters dependent on the soil or crop water status.

Transpiration fluxes can be therefore determined multiplying the maximum crop transpiration for a water stress coefficient, depending on the soil/plant water status and on environmental variables.

Several models have been proposed to quantify the water stress coefficient as a linear or nonlinear function of the soil water status, expressed in terms of matric potential (Feddes, 1978; van Genuchten, 1987; Dirksen, 1993; Homaee, 1999) or soil water depletion (Steduto 2009).

For a certain crop the water stress function can be defined once it is known its shape and the thresholds values of soil water content or matric potential representing, from one side, the soil water status beyond which crop water stress occurs and, from the other, the condition of maximum stress.

With reference to the critical thresholds of soil water status on Olive orchards, Fernández and Moreno (1999) observed the absence of crop water stress in the range of the available water between 1 and 0.4. This condition was recognized according to values of pre-dawn xylematic and stems water potential around -0.46 MPa and -1.3 MPa respectively. In the same experiments, the maximum water stress condition was determined as corresponding to soil matric potential lower than -1.5 MPa, usually considered the wilting point for other fruit tree species.

Even if various linear and nonlinear functions, aimed to relate the water stress coefficient to the soil/plant water status, have been proposed for different crops (Ahuja et al., 2008), there is a lack of knowledge on the shape of the water stress function valid for olive orchards, so that field specific investigations are required.

In this context, the main objective of the work is to assess the shape of the water stress function for table olive orchards. Such function has been expressed as a relationship between the relative transpiration and the soil water status identified as soil matric potential or, alternatively, between the leaf/stem water potential and the relative depletion.

Moreover, critical thresholds of soil water status were identified according to measured soil m atric potentials and leaf/stem xylematic potentials and used to determine the water stress function parameters.

Modelling Plant Water Stress Response

Under stress conditions, olive crop develops different adaptive strategies: i) reducing the water content/xylematic potential of its tissues, in order to increase the gradient of potential between soil and leaves; ii) limiting the plant grow without stopping its photosynthetic activity; iii) adjusting the osmotic potential, so that the cellular turgor and the leaf activities are maintained (Xiloyannis et al., 1999).

Despite the complexity of the olive response to soil water deficit, the spatial distributions of roots and soil water content play an important rule on stomatal conductance and leaf water status. This circumstance suggests the use of the macroscopic approach to assess the water stress function as a reduction term of potential transpiration, that can be defined as:

$$\alpha = \frac{T_a}{T_p} = f\left(\text{soil/plant water status}\right) \tag{1}$$

where T_a and T_p are the actual and potential transpiration and f is a function of soil/plant water status, i.e. soil water content, soil matric potential, leaf/steam xylematic potential, etc. Once the potential transpiration is determined, the knowledge of α allows the estimation of the actual transpiration T_a.

Potential transpiration, T_p, can be estimated by following the procedure suggested by Jarvis and McNaughton (1986):

$$T_p = \frac{\Delta R + \dfrac{\rho C_p VPD}{r_a}}{\lambda\left[\Delta + \gamma\left(\dfrac{r_a + r_{c,\min}}{r_a}\right)\right]} \tag{2}$$

where Δ [kPa C^{-1}] is the slope of the saturation vapor pressure curve, R [W m^{-2}] is the net radiation, ρ [Kg m^{-3}] is the air density, C_p [J Kg^{-1} K^{-1}] the air specific heat at constant pressure, γ [KPa K^{-1}] is the psychometric constant, VPD [kPa] is the air vapor pressure deficit, λ [J Kg^{-1}] is the latent heat of vaporization, r_a and $r_{c,\min}$ are the aerodynamic and the minimum canopy resistance, respectively.

All the variables in eq. 2 can be obtained from the recorded meteorological data, except r_a and r_c, requiring more complicated computations.

Assuming a logarithmic wind profile, the aerodynamic resistance, r_a [s m^{-1}], for neutral conditions, can be evaluated with an expression derived from turbulent transfer, (Perrier, 1975):

$$r_a = \frac{\ln\left[\frac{(z-d)}{z_{om}}\right]\ln\left[\frac{(z-d)}{(h_c-d)}\right]}{k^2 u_z} \tag{3}$$

where z [m] is the reference level at which the wind speed u_z [m s^{-1}] is measured and z_{om} =0.123h_c [m] is the roughness length for momentum, h_c [m] is crop height, k (=0.41) is the von Karman's constant equal to 0.41, d =0.667h_c [m] is the zero plane displacement height.

On the other hand, values of r_c can be obtained by means of a physically-based approach, as (Berni et al., 2009):

$$r_c = \frac{r_a\left(e_c^* - e_a\right)}{\gamma\left[\frac{r_a R}{\rho c_p} - (T_c - T_a)\right]} - r_a \tag{4}$$

where e_c^* is the saturated vapor pressure at the canopy temperature, T_c, and e_a is the actual vapor pressure.

A rather simple approach to evaluate α, as a function of soil water pressure head, has been proposed by Feddes et al., (1978):

$$\alpha(h) = \frac{h - h_4}{h^* - h_4} \tag{5}$$

where h^* is a threshold value of the matric potential depending on the transpirative atmospheric demand and h_4 is the matric potential corresponding to the wilting point. This model describes the water stress through a linear function, so that the actual transpiration linearly decreases with α, in the range $h_4<h< h^*$.

The shape of transpiration reduction function depends on several factors and in particular on the eco-physiological processes, like plant resistance/tolerance/avoidance to water stress (Larcher, 1995), as well as on soil water availability in the root zone (Guswa et al, 2004).

Convex $\alpha(h)$ curves are typical of xerophytes, for which the reductions of actual transpiration becomes severe only for extreme water stress. On the other hand concave shapes of the $\alpha(h)$ relationship, denote strong reductions of actual transpiration, even for slight stress levels.

The shape of the stress function can be taken into account by introducing an exponent, a, to the right side member of eq. 5:

$$\alpha(h) = \left(\frac{h - h_4}{h^* - h_4}\right)^a \tag{6}$$

Values of $0<a<1$ define convex shapes, whereas values of $a>1$ reproduce concave shapes.

Another non-linear $\alpha(h)$ model was proposed by van Genuchten (1987):

$$\alpha(h) = \frac{1}{1+\left(\frac{h}{h_{50}}\right)^p} \qquad (7)$$

where h_{50} is the soil matric potential for which α=0.5 and p is a dimensionless parameter depending on crop, soil, and climate (Homaee, 1999).

Dirksen et al. (1993) modified eq. 7, in order to assume that root water uptake decreases when soil matric potentials is lower than a threshold value h^*:

$$\alpha(h) = \frac{1}{1+\left[\frac{\left(h^*-h\right)}{\left(h^*-h_{50}\right)}\right]^p} \qquad (8)$$

Homaee (1999) replaced, in eq. 8, h_{50}, with h_{max}, to take into account the soil matric potential beyond which the changes of h no longer significantly influence the relative transpiration and introduced a second parameter, α_0, representing the relative transpiration at h_{max}, so that:

$$\alpha(h) = \frac{1}{1+\frac{\left(1-\alpha_0\right)}{\alpha_0}\left[\frac{\left(h^*-h\right)}{\left(h^*-h_{\max}\right)}\right]^p} \qquad (9)$$

Recently Steduto et al. (2009) proposed a new model, describing the stress coefficient, α, as a function of the relative depletion (D_{rel}), defined in the domain of soil water contents determining stress conditions for the crop ($\theta^*<\theta<\theta_{min}$):

$$\alpha\left(D_{rel}\right) = 1-\frac{e^{D_{rel}\, f_s}-1}{e^{f_s}-1} \qquad (10)$$

where f_s is a parameter defining the shape of the stress function. This function is linear for f_s tending to 0, concave for $f_s<0$, and convex for $f_s>0$.

The relative depletion can be evaluated as:

$$D_{rel} = \frac{\theta^*-\theta}{\theta^*-\theta_{\min}} \qquad (11)$$

where θ^* is the threshold value of the soil water content below which water stress occurs and $\theta_{\min}$ corresponds to the soil water content for which the stress is at its full strength.

According to eq. 11, water stress starts when $D_{rel}>0$ ($\alpha<1$); at the lowest water content (θ_{min}), the effect of water stress is extreme ($D_{rel}=1$; $\alpha=0$).

For each value of the relative depletion, the stress coefficient α can be evaluated in terms of leaf/steam water potentials or stomatal conductance (Raes, 2008). Whatever eco-physiological variable is used, it is necessary to normalize its measured value to a fractional scale variable in the range 0-1.

Considering that all the described stress functions are empirical, the upper and lower thresholds of soil/crop water status must be locally determined, in order to take into account the crop, the climate and the soil properties. Moreover, for each soil-crop system the parameters of the stress functions must be determined.

Materials and Methods

Site descriptions and experimental layout

Experiments were carried out during irrigation seasons 2008 and 2009 (from June to September), in the farm "Tenuta Rocchetta" located near Castelvetrano (TP), in SW of Sicily (Lat. 37° 38' 36,8", Long. 12° 50' 49,8").

The farm, having an extension of about 13 ha, is mostly cultivated with table olive grove (*Olea europaea* L., var. Nocellara del Belice), representing the main crop in the surrounding area. The experimental plot is characterized by 15 years old olive trees, planted on a regular grid of 8 x 5 m (250 plants/ha); the mean canopy height is about 3.7 m and the average fraction of vegetation cover is about 0.35. Irrigation is practiced by means of a drip irrigation system, with four 8 l/h emitters per plant. Soil texture was measured using the hydrometer method on the same soil samples used for the water retention curves. Soil textural class, according USDA classification, is silty clay loam.

Meteorological data (incoming short-wave solar radiation, air temperature, air humidity, wind speed and rainfall) were hourly collected by SIAS (Servizio Informativo Agrometeorologico Siciliano), with standard equipments installed about 500 m apart from the experimental field.

A preliminary investigation on the root spatial distribution was carried out in order to identify the soil volume with the highest root density, where the water uptake processes are concentrated. Vertical and horizontal Root Length Density (*RDL*) were determined on sixten vertical profiles opened according to a regular grid, where 96 soil carrots (5 cm diameter and 15 cm high) were collected at depths of 30, 45, 60, 75, 90 and 100 cm. Root extraction procedure followed the protocol proposed by Newman, (1966). Fig. 1 shows, per each investigated layer, a 2D map of the normalized *RDL* values. As can be observed at each depth the highest root density is localized in the soil volume wetted with irrigation.

Investigation allowed to identify two soil volume explored by roots (Xiloyannis et al., 2012): the first where most of the root absorption takes place, corresponding to the soil volume wetted during irrigation, whereas the second volume, also explored by roots, is not wetted during irrigation. According to the experimental results the soil volume where 80% of roots are localized, can be assumed as a parallelepiped having a length equal to the tree spacing (5.0 m), a width of 1.5 m and a depth of 0.75 m.

The knowledge of the dimensions of the soil volume where root water extraction occurs allowed to identify where to collect the soil samples used to determine the soil water retention curves and to install the sensors to measure the soil water contents.

Soil water retention curves were determined on eight undisturbed soil samples, 0.08 m diameter and 0.05 m height, collected at depth of 0, 30, 60 and 100 cm. Hanging water column apparatus (Burke et al., 1986) was used to evaluate soil water contents corresponding to h values ranging from -0.05 to -1.5 m; pressure plate apparatus (Dane and Hopmans, 2002), with sieved soil samples 0.05 m diameter and 0.01 m height, was used to determine soil water contents corresponding to h values of -3.37 m, -10.2 m, -30.6 m, and -153.0 m. For each undisturbed sample dry bulk density, ρ_b, [Mg m^{-3}] was also determined.

The van Genuchten model (van Genuchten, 1980) was used to fit experimental data; the water retention curve parameters were obtained by means of the retention code (RETC, van Genuchten et al., 1992).

Fig. 2 shows the soil water retention curves obtained for the investigated layers, whose van Genuchten parameters are shown in Tab. 1. Considered the low differences between soil water contents measured at the different layers, for each fixed matric potential, an averaged soil water retention curve was used for the following analysis.

Irrigation scheduling followed the ordinary management practised in the surrounding area. The total irrigation depth provided by the farmer was equal to 122 mm, divided in four waterings, in 2008 and 127 mm, divided in five waterings, in 2009. Tab. 2 shows the irrigation calendar and the rainfall depths during the investigation periods, from July, 1, 2008 to August, 31 of 2008 and 2009.

In order to evaluate the water stress thresholds and to estimate the model fitting parameters at the scale of a single plant, experiments were carried out by monitoring, during a dry period, the evolution of the considered water stress coefficients, $\alpha(h)$ or $\alpha(D_{rel})$, and the corresponding soil water status, described in terms of h or D_{rel}.

Measurements of soil and plant water status

Spatial and temporal variability of soil water contents was monitored, from the soil surface to a depth of 100 cm, using a Diviner 2000 Sentek FDR (Frequency Domain Reflectometry) probe. The access tubes have been placed in the soil volume where 80% of roots were localized. The probe containing the sensor, when inserted in the access tube, allows to measure soil water content at the different depths. Before using the probe it was necessary to proceed to a site specific calibration, aimed to determine the relationship between the Scaled Frequency, SF, measured by the probe and the volumetric soil water content, θ.

Five access tubes were installed along the direction of the irrigation pipeline, between two consecutive trees and where the highest change of soil water content occurred. In this way it was possible to take into account the spatial variability of soil water content after irrigation. Soil water contents measurement were carried out every five days, as well as before and after each watering.

In 2009 season, additional measurements of soil water contents were carried out using TDR (Time Domain Reflectometry) probes connected to a multiplexer. Six probes, 20 cm length, were installed between two consecutive trees along the direction of the irrigation pipeline, at distances of 50, 100 and 250 cm from the tree, in the layer 5-25 cm and 40-60 cm.

Values of soil water contents measured with FDR and TDR systems were then averaged proportionally to the spatial root density experimentally measured, in order to determine, for each measurement day, a single value of θ, representative of the soil layer where most of the root absorption takes place.

For each soil water content, θ, the relative depletion can be determined with eq. 11, once the threshold values of the soil water content, θ^* and $\theta_{\min}$, are known.

Sap fluxes were measured hourly, on three olive trees, by thermal-based sensors, using two standard Thermal Dissipation Probes, TDPs (Granier, 1987) per each tree. As suggested by the manufacturer, the probes were implanted 22 cm deep, in order to sample only the conductive area. After installing the probes, the trunk was wrapped in reflective insulation. Each hour the temperature difference between the heated upper needle and the un-heated lower needle, combined with the temperature difference at night allowed to estimate the sap velocity, that was then multiplied to the sapwood area in order to obtained hourly sap fluxes.

At the end of the experiments, the sapwood area was determined by a colorimetric method, on a total of six wood carrots extracted on the same three trees, in between each couple of the sap flow probes, with a Pressler gimlet. The conductive section was identified by adding methyl-orange to the carrot, in order to enhance the difference between the sapwood and the heartwood. Each image of colored wood carrot was then analyzed with software Image-Pro Plus 6.0 to recognize the sapwood depth. The fluxes were then integrated on a daily scale in order to evaluate the volume of water consumed by each plant.

The actual daily stand transpiration, T_a (mm d^{-1}), was then obtained by scaling up the sap fluxes taking into account the pertinence area of a single plant (40 m^2), under the hypotheses of neglecting, at a daily scale, the tree capacitance.

In order to estimate T_p by means eq. 2, values of net radiation R were continuously monitored with a 4-component net-radiometer (NR-01, Hukseflux™ Thermal Sensors), installed 6 m apart from the investigated trees. The minimum value of the canopy resistance, $r_{c,min}$, has been calculated applying eq. 4 through measurement of canopy temperature at midday, with a hand held infrared thermometer, carried out on 3 additional fully irrigated olive plants. In order to reduce the possible direct soil thermal effect, for each tree, 6 values of canopy temperature were randomly acquired by the side of the cardinal directions.

A number of two replicates of predawn leaf water potential, (*PLWP)*, midday leaf water potential (*MLWP*) and midday stem water potential (*MSWP*) were measured by using a pressure chamber (Scholander et al., 1965) with the protocol proposed by Turner e Jarvis (1982), in the same three trees, where soil water status and sap fluxes were monitored. In particular, *PLWP* measures the plant water status at theoretical (or nominal) zero plant water flux and provides information on soil water potential in the root zone as a consequence of the equilibrium between soil and atmosphere. *MLWP*, measured on a single leaf, reflects the combination of local factors like leaf water demand, vapor pressure deficit (*VPD*), leaf intercepted radiation, soil water availability, internal plant hydraulic conductivity and stomatal regulation, whereas *MSWP*, measured on a non-transpiring steam (Begg and Turner, 1970) mainly depends on the soil water status.

For each tree, the values of leaf water potentials were measured on one-year-old shoots, whereas *MSWP*s were measured on leaves that were covered with foil faced bags, after at least 30 minutes prior to measurements to allow equilibration. Measurements were carried out every five days, as well as during the days immediately before and after irrigation.

Results and Discussions

A preliminarily investigation was carried out in order to proceed to the site-specific calibration of the FDR sensor. The following function was in particular obtained for the investigated soil site (R^2= 0.92; RMSE=0.03 $cm^3\ cm^{-3}$):

$$\theta = 38.225\ SF^{3.4918} \qquad (12)$$

The thermal measurements performed over well watered plants allowed to estimate the minimum value of the canopy resistance, $r_{c,min}$ [s^{-1} mm], necessary to compute the potential transpiration, T_p (eq. 2). For the considered periods, the average minimum value of canopy resistance, $r_{c,min}$, evaluated with eq. 4, resulted equal to 76±5 s m-1.

For the constantly irrigated plants, tab. 3 shows the minimum and maximum values of the meteorological variables, as well as of soil water content, predawn leaf water potential and canopy temperature, recorded during the investigated periods.

According to the *PLWP* threshold values suggested by Fernandez and Moreno (1999), the monitored plants were practically maintained under conditions of absence or moderate water stress (*PLWP* ≥-0.5 MPa).

Plant-Soil water relationships and definition of critical thresholds

Fig. 3 illustrates the actual transpiration, T_a, and the corresponding absolute values of *PLWP*, *MLWP* and *MSWP*. As can be observed actual transpiration is strongly correlated with all the considered independent variables. Moreover a decreasing trend of actual transpiration is evident at increasing absolute values of leaf or stem water potential.

Considering the high correlations observed between T_a and plant water status identified through the leaf water potentials, an analysis was carried out in order to find the critical soil water status conditions identifying the begin and the maximum crop water stress.

Soil water status was expressed in terms of volumetric soil water content, θ, and soil matric potential, *h*. While the first variable gives site-specific indications, the second is associated to the capacity of soil to hold water and therefore it can be considered as a status variable for the investigated crop.

Fig. 4 shows the values of actual transpiration as a function of the average soil water content measured in 2008 and 2009 with the FDR technique, in the layer 10-100 cm. The figure also represents the average water retention curve. Despite the limited number of T_a measurements corresponding to high water contents, values of actual transpiration can be considered practically constant for soil water contents higher than a threshold value and drastically decreases for lower values. According to the experimental data, the critical average soil water content below which is recognizable a strong reduction of actual transpiration is approximately equal to 16±2%. The variability of this threshold certainly depends on the atmospheric water demand.

The corresponding value of critical soil matric potential is around 40 m, with values in the range 20-90m. This recognized large range is obviously consequent to the high change of soil matric potential corresponding to limited variations of soil water content. For soil water content higher than the critical value, actual transpiration is more or less constant and equal approximately to 2 mm d^{-1}, whereas for lower water contents, actual transpiration drop off to a minimum value of about 0.7 mm d^{-1}.

A similar trend is obtained when considering both FDR and TDR data in the layer 45-65, where the highest root density is concentrated. Fig. 5 illustrates the values of actual transpiration as a function of the average soil water contents in the soil layer 45-65 cm, measured with both FDR and TDR techniques, the average water retention curve in the considered soil layer, as well as the range of variation of the observed critical thresholds of soil water content/matric potential.

Fig. 6a-c shows the experimental values of *PLWP*, *MLWP*, *MSWP* and the corresponding soil water contents, averaged for the root density, in the layer 10-100 cm. As can be observed in fig.6a, the values of *PLWP* follow the same trend recognized for T_a.

Despite it was quite difficult to identify an unambiguous threshold of soil water content, due to the visible dispersion, the critical value of θ^*≈16% (h ≈ 40 m) previously obtained, was considered acceptable. The observed uncertainty could be due to xilematic potentials adjustment occurring when the plant is kept under soil water deficit for long time periods, as well as to the different climatic conditions recorded during the experiments.

The critical value θ^* separates two different plant behaviors: for $\theta>\theta^*$, the absolute values of *PLWPs* are constant and approximately equal to 0.5 MPa, identifying a condition of negligible water stress (Fernandez and Moreno, 1999). On the other hands, for $\theta<\theta^*$, lower is the soil water content, smaller is the *PLWP*, as consequence of the progressively increasing water stress. Similar results can be observed when *MLWP*s and *MSWP*s are considered in place of *PLWP*s.

The higher dispersion observable for $\theta>\theta^*$, when *MLWP* or *MSWP* are considered, can be explained by the dependence of the midday potentials from the environmental variables. However, under water stress conditions ($\theta<\theta^*$), whatever potential is used, the dispersion is comparable as consequence of the minor influence of the environmental variables.

Experimental data represented in fig. 6 a-c provides also a clear identification of the soil water status corresponding to the maximum recognized water stress level.

In fact, as can be observed in fig. 6a, the maximum measured value of the *PLWP* of 2.1 MPa corresponds to a soil water content slightly higher than 11% and consequently to a matric potential of about h=200 m. This value of soil matric potential was assumed corresponding to h_4 (eqs. 5 and 6) or h_{max} (eq. 9) and represents the minimum thresholds of soil water status, identifying the most extreme water stress condition recognized in the field.

Modeling olive response to soil water deficit

According to the procedure proposed by Ewers and Oren (2000), to keep errors in T_p to less than 10%, estimated T_p have to be limited to conditions for which $VPD \geq 0.6$ kPa. For this reason, it was therefore necessary to proceed to a data screening, in order to neglect all the environmental condition determining $VPD \geq 0.6$ kPa.

Considering that the water stress conditions were observed in the range of soil matric potential absolute values between 40 m and 200 m, the estimation of model parameters (a, p, α_0) was consequently carried out by assuming the first value as the threshold of soil matric potential (h_3 or h) below which the plant starts to reduce transpiration ($T_a\ T_p^{-1} < 1$) and the second value was considered as the soil matric potential (h_4 or h_{max}) corresponding to absence of transpiration. Moreover, considering the minimum α observed in the field was equal to 0.6, the threshold h_{50} of eqs. 7 and 8, was assumed equal to 152 m , corresponding to α=0.6, rather than 0.5.

For all examined models, tab. 4 shows the critical thresholds of soil water status as well as the relative parameters obtained by fitting the data with a least square method, by using the package Excelstat (Addinsoft USA, 2010) and the Pearson correlation coefficient.

Fig. 7 a-b shows the h, $T_a\ T_p^{-1}$ experimental data pairs as well as the fitting models (eqs. 5 to 9), whose critical thresholds and parameters are indicated in tab. 4. Analysis of data evidenced that non-linear water stress models better reproduce the initial phase of the transpiration reduction process, compared to the linear model. The convex shape of the stress function evidences that water stress is more and more severe at increasing matric potential, and therefore the reduction of actual transpiration becomes critical only for the most extreme water stress conditions. For this reason, Feddes $\alpha(h)$ linear model, defined by only the measured critical thresholds of soil matric potential (h^*, h_4), gives the worst result, because it does not allow to take into account the convex shape of the function.

Unfortunately, the absence of measurements for $T_a\ T_p^{-1}$ lower than 0.6, does not permit to clearly choose the best shape describing the olive response to more severe water stress conditions than those observed. However under the examined field conditions it was very difficult to reach values of $T_a\ T_p^{-1}$ lower than 0.6, considering that: i) the high capacitance characterizing the olive plants, like those observed, allows them a certain adaptation to water stress conditions; ii) investigated soil is characterized by high water retentivity; iii) the distances between the plants allow a large soil volume for root absorption.

Accounting for the similar statistical significance of the examined non linear models (eqs. 7 to 9), the one requiring the knowledge of a single parameter should be preferred (eq. 7). However, further investigations aimed to explore a more extent range of $T_a\ T_p^{-1}$ values could allow a better modeling of the stress function under higher water stress levels.

The values of the stress coefficient α in eq. 10 were determined considering, as indicators, both the measured *PLWP* and *MSWP* values, normalized respect of their domain limits. On the other hand the values of D_{rel} were obtained using eq. 11, considering θ^*=0.16 cm^3 cm^{-3} (D_{rel}=0) and θ_{min}=0.11 cm^3 cm^{-3} (D_{rel}=1), as previously discussed.

Fig. 8 a-b shows α, D_{rel} data pairs experimentally determined, the fitted water stress model, as well as the values of the model parameter f_s.

As can be observed in fig. 8 the shape of the represented model is still convex, as consequence of f_s>0 for both cases. Despite the similar *RMSE* values, the slightly higher dispersion visible when the *MSWPs* are considered is a consequence of the sensitivity of the measurements from the variation of the environmental variables.

Whatever water stress model is considered therefore, for the examined crop, the shape of the stress function is always convex.

Conclusions

Critical thresholds of soil water status identifying olive crop response to water stress were determined and the performance of existing model of the stress function analyzed. The experiments evidenced in particular a first critical soil water content θ^*=0.16 cm^3 cm^{-3}, corresponding to a soil matric potential of about 40 m, separating two different plant behaviours: for $\theta > \theta^*$, where the absence of water stress was detected, actual transpiration resulted constant and approximately equal to 2 mm d^{-1}, while for $\theta < \theta^*$, crop water stress increases at decreasing θ. On the other side, the extreme crop water stress was recognized when soil water content was about 0.11 cm^3 cm^{-3}, and soil matric potential of about 200 m. Under this last condition actual transpiration resulted about 60% of its corresponding potential value.

With the exception of the Feddes linear model, for which it is not possible to consider the shape of the stress function, all the other investigated models showed a good agreement with the experimental data.

Non-linear models, in fact, better reproduce the initial phase of the transpiration reduction process, showing that for olive groves the stress function has a convex shape, for which the reduction of actual transpiration is significant only under extreme water stress conditions. Unfortunately, the absence of relative transpiration lower than those observed in the field, does not allow to choose the best model representing the shape of the stress function under very low soil water contents.

Acknowledgements

Research was carried out within the project PRIN 2008 (Provenzano), co-financed by Ministero dell'Istruzione, dell'Università e della Ricerca (MIUR) and Università degli Studi di Palermo.

Author’s Contribution

Contribution to the paper has to be shared between Authors as following: Field data collection and data processing were cared by G. Rallo. Set-up of research, discussion of results and final revision of the text have to be equally divided between all the Authors. Text was written by G. Rallo and G. Provenzano.

References

Ahuja, L.R, Reddy, V.R., Saseendran, S.A., Yu, Q. 2008. Response of Crops to Limited Water: Understanding and Modeling Water Stress Effects on Plant Growth Processes. Complete Book. ASA, CSSSA and SSSA, Madison, Wisconsin. 436 pp.

Begg, J.E., Turner, N.C., 1970. Water potential gradients in field tobacco. Plant Phys. 46, 343-346.

Berenguer, M.J., Vossen, P.M., Grattan, S.R., Connell, J.H., Polito, V.S. 2006. Tree irrigation levels for optimum chemical and sensory properties of olive oil. Hortic. Sci. 41, 427-432.

Berni, J.A.J., Zarco-Tejada, P.J., Sepulcre-Cantó, G., Fereres, E., Villalobos, F. 2009. Mapping canopy conductance and CWSI in olive orchards using high resolution thermal remote sensing imagery. Remote Sens. Environ., 113, 11.

Burke, W., Gabriels, D., Bouma, J., 1986. Soil structure assessment. Rotterdam, The Netherlands: Balkema.

Cammalleri, C., Anderson, M.C., Ciraolo, G., D'Urso, G., Kustas, W.P., La Loggia, G., Minacapilli, M. 2010b. The impact of in-canopy wind profile formulations on heat flux estimation in an open orchard using the remote sensing-based two-source model. Hydrol. Earth Syst. Sci. 14(12), 2643-2659.

Cammalleri C., Agnese C., Ciraolo G., Minacapilli M., Provenzano G., Rallo G. 2010. Actual evapotranspiration assessment by means of a coupled energy/hydrologic balance model: Validation over an olive grove by means of scintillometry and measurements of soil water contents. J. of Hydr. 392(1-2), 70-82.

Caruso, G., Gucci, R., Rapoport, H.F. 2011. Deficit irrigation effects on yield components of Olive trees during the onset of fruit production. Acta Hort. (ISHS). 889, 291-296.

D'Andria, R., Lavini, A., Morelli, G., Patumi M., Terenziani, S., Calandrelli, D., Fragnito, F. 2004. Effect of water regime on five pickling and double aptitude olive cultivars (Olea europaea L.). J. Hortic. Sci. & Biotech. 78(1), 15-23.

Dane, J.H, Hopman, J.W., 2002. Water retention and storage. In: Dane J,H,, Topp G,C, (eds) Methods of soil analysis: Part 4-Physical methods. SSSA Book Ser. 5. SSSA, Madison.

Dirksen, C., Kool, J.B., Koorevaar, P., van Genuchten, M.T. 1993. Hyswasor: Simulation model of hysteretic water and solute transport in the root zone. In: Russo D. and Dagan G. (Eds.), Water flow and solute transport in soils. Springer-Verlag, Adv. Series in Agric. Sci. 20, 99-122.

Ewers, B.E., Oren, R. 2000. Analysis of assumptions and errors in the calculation of stomatal conductance from sap flux measurements. Tree Phys. 20, 579-590.

Feddes, R.A., Kowalik, P.J., Zaradny, H. 1978. Simulation of field water use and crop yield. Simulation Monographs. Pudoc, Wageningen. 189 pp.

Fernadez, J.E., Moreno, F. 1999. Water use by Olive tree. J. Crop Prod. 2, 101-162.

Fernández, J.E., Díaz-Espejo, A., Infante, J.M., Duran, P., Palomo, M.J., Chamorro, V., Girón, I.F., Villagarcía, L., 2006. Water relations and gas exchange in olive trees under regulated deficit and partial root zone drying. Plant Soil. 284, 273-291.

Granier, A. 1987. Evaluation of transpiration in a Douglas-fir stand by means of sap flow measurements. Tree Phys. 3, 309–320.

Guswa, A.J., Celia, M.A., Rodriguez-Iturbe, I. 2004. Effect of vertical resolution on predictions of transpiration in water-limited ecosystems. Adv. Water Res. 27, 467–480.

Homaee, M. 1999. Root water uptake under non-uniform transient salinity and water stress. Ph.D. dissertation. Wageningen Agric. Univ., Wageningen, The Netherlands, 173 pp.

Jarvis, P.G., Mc Naughton, K.G. 1986. Stomata control of transpiration: Scaling up from leaf to region. Adv. Ecol. Res. 15, 1-49.

Larcher, W. 1995. Physiological plant ecology. Springer-Verlag, Berlin. 488 pp.

Newman, E I. 1966. A method of estimating the total length of root in a sample. J. Appl. Ecol. 3, 139-145.

Minacapilli, M., Iovino, M., D'Urso, G. 2008. A distributed agro-hydrological model for irrigation water demand assessment. Agric. Water Manage. 95(2), 123-132.

Minacapilli, M., Agnese, C., Blanda, F., Cammalleri, C., Ciraolo, G., D'Urso, G., Iovino, M., Pumo, D., Provenzano, G., Rallo, G.. 2009. Estimation of Mediterranean crops evapotranspiration by means of remote-sensing based models. Hydr. and Earth System Sci. Vol. 13, 1061-1074.

Patumi, M., D'Andria, R., Fontanazza, G., Morelli, G., Giorio, P., Sorrentino, G. 1999. Yield and quality traits of three intensively trained olive trees cv. under different irrigation regimes. J. Hortic. Sci. & Biotech. 74, 729-737.

Patumi, M., D'Andria, R., Marsilio, V., Fontanazza, G., Morelli, G., Lanza, B. 2002. Olive and Olive oil quality after intensive monocone olive growing (Olea europaea L., cv. Kalamata) in different irrigation regimes. Food Chem. 77, 27-34.

Perrier, A. 1975. Etude de l'evapotranspiration dans les condition naturelles. I. Evaporation et bilan d'energie des surfaces naturelles. Ann. Agron. 26, 1-18.

Personne, E., Perrier, A., Tuzet, A. 2003. Simulating water uptake in the root zone with a microscopic-scale model of root extraction. Agronomie 23, 153-168.

Raes, D. 2008. Deficit irrigation strategies via crop water productivity modelling: Field research of quinoa in the Bolivian altiplano. PhD thesis diss., Katholieke Universiteit Leuven. 237 pp.

Rallo G., Agnese, C., Minacapilli, M., Provenzano, G. 2012. Comparison of SWAP and FAO Agro-Hydrological Models to Schedule Irrigation of Wine Grape. Journal of Irrigation and Drainage Engineering, Vol. 138(7), 581-591.

Rousseaux, M.C, Figuerola, P.I., Correa-Tedesco, G., Searles, P.S. 2009. Seasonal variations in sap flow and soil evaporation in an olive (Olea europaea. L) grove under two irrigation regimes in an arid region of Argentina. Agric. Water Manage. 96, 1037-1044.

Scholander, R.R., Hammel, H.T., Bradstreet, E.D., Hemmiegsen, E.A., 1965. Sap pressure in vascular plants. Science. 148, 339-346.

Skaggs, T.H., van Genuchten, M.T., Shouse, P.J., Poss, J.A., 2006. Macroscopic approaches to root water uptake as a function of water and salinity stress. Agric. Water Manage. 86, 140-149.

Steduto, P., Hsiao, T.C., Raes, D., Fereres, E. 2009. AquaCrop. The FAO crop model to simulate yield response to water. Reference Manual.

Tognetti, R., d´Andria, R., Morelli, G., Calandrelli, D., Fragnito, F. 2004. Irrigation effects on daily and seasonal variations of trunk sap flow and leaf water relations in olive trees. Plant Soil. 263 (1-2), 249-264.

Turner, M.T., Jarvis, G.P. 1982. Measurement of plant water status by the pressure chamber technique. Irrig. Sci. 9, 289-308.

van Genuchten, M.T., 1980. A closed-form equation for predicting the hydraulic conductivity of unsaturated soils. Soil Sci. Am. J. 44, 892-898.

van Genuchten, M.T., 1987. A numerical model for water and solute movement in and below the root zone. Reserch Report, US Salinity Lab., Riverside, CA.

van Genuchten, M.T., Leij, F.J., Yates, S.R. 1992. The RETC code for quantifying the hydraulic functions of unsaturated soils. Project summary, EPA'S Robert S. Kerr Environmental Research Lab., Ada ,OK, USA.

Xiloyannis C., Dichio B., Nuzzo, V., Celano G. 1999. Defence strategies of olive against water stress. Acta Hort. 474, 423-426.

Xiloyannis, C., Montanaro, G., Dichio, B. 2012. Irrigation in Mediterranean Fruit Tree Orchards. In: Irrigation Systems and Practices in Challenging Environments. Teang Shui Lee Ed., ISBN 978-953-51-0420-9.

*Abstract
Click here to download Abstract: ABSTRACT.pdf

Abstract

Crop response to water stress is very important to predict transpiration reductions under limited soil water conditions and it can be evaluated according to global stress indicators like relative transpiration or xylematic water potential. Assessing empirical functions able to describe the plant response to water stress, on the basis of parameters depending on the soil or crop water status, is crucial for a rational scheduling of irrigation.

In order to assess whatever water stress model, it is necessary to estimate critical thresholds of soil water status, below which plant transpiration starts to decrease.

The main objective of the work is to identify the shape and to determine the parameters of table olive orchards water stress function, assessed according to relative transpiration or leaf/stem water potential.

The study area, located in the South-Western coast of Sicily (Italy), where table olive orchards are the principal crop, is characterized by typical Mediterranean semi-arid climate. Experiments were carried out during irrigation seasons 2008 and 2009 in a farm mainly cultivated with olive grove (*Olea europaea*, var. Nocellara del Belice) with plants of about 15 years old, spaced 8 m x 5 m. Irrigation water was supplied by means of a drip system, with irrigation timing and doses scheduled according to the ordinary management of the area.

Meteorological data were collected by a weather station located nearby the experimental lay-out.

The collected data allowed to assess different water stress functions describing the crop eco-physiological field response to soil water status.

Thresholds of soil water content and matric potential below which actual transpiration decreases with soil water content were obtained. For values of soil water contents higher than the critical threshold, actual transpiration resulted almost constant. A similar behavior was observed when the xylematic leaf/stem water potentials were used to quantify the crop water stress. Investigation also showed that the non-linear models better reproduced the initial phase of the transpiration reduction process; for the examined crop, in fact, convex shape models typical of xerophytes, better reproduced the reductions of actual transpiration under the soil water deficit conditions recognized in the field.

Figure1

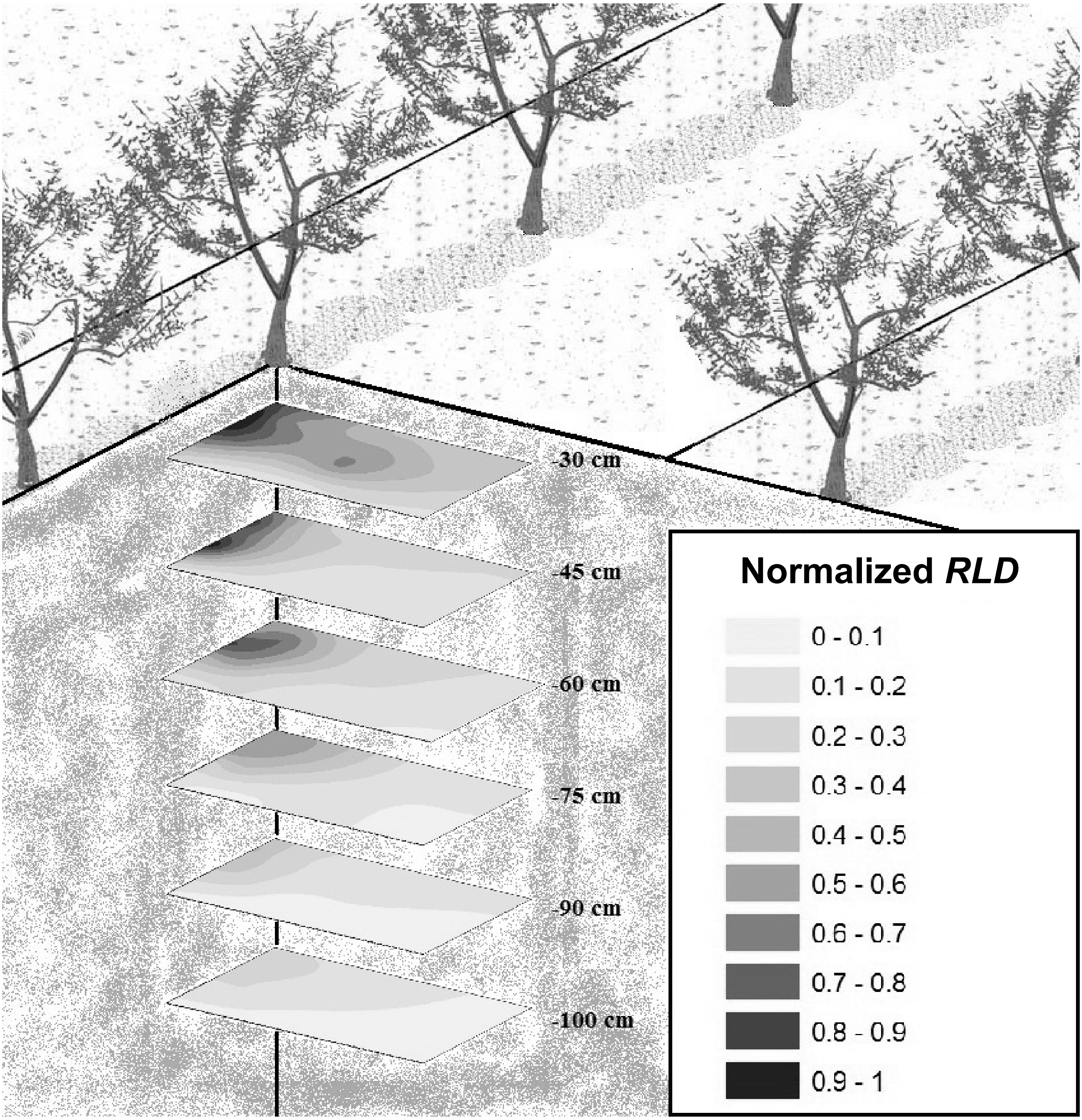

-30 cm
-45 cm
-60 cm
-75 cm
-90 cm
-100 cm
Normalized *RLD*
0 - 0.1
0.1 - 0.2
0.2 - 0.3
0.3 - 0.4
0.4 - 0.5
0.5 - 0.6
0.6 - 0.7
0.7 - 0.8
0.8 - 0.9
0.9 - 1

Figure2

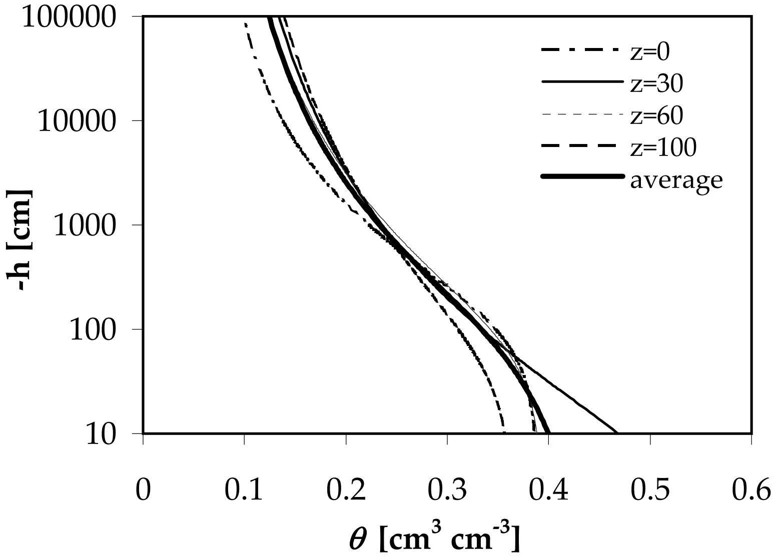

100000
10000
1000
100
10
-h [cm]
0
0.1
0.2
0.3
0.4
0.5
0.6
θ [cm3 cm-3]
z=0
z=30
z=60
z=100
average

Figure3

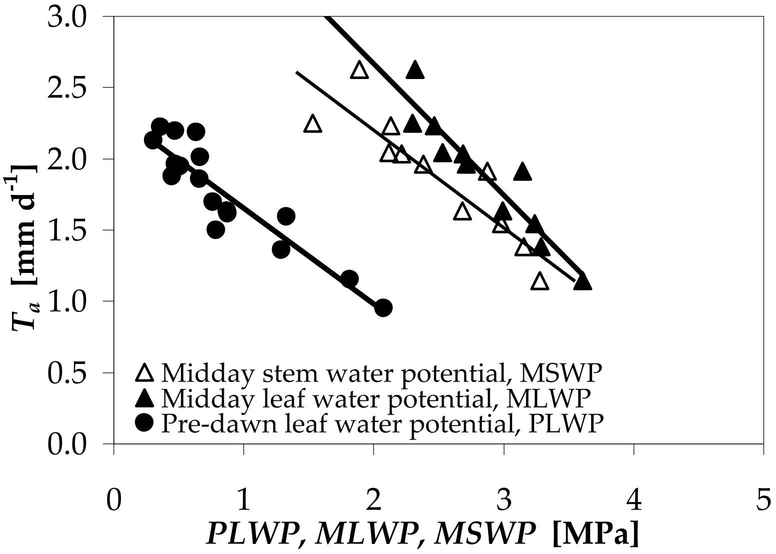
3.0
2.5
2.0
1.5
1.0
0.5
0.0
T_a [mm d^{-1}]
Midday stem water potential, MSWP
Midday leaf water potential, MLWP
Pre-dawn leaf water potential, PLWP
0
1
2
3
4
5
PLWP, MLWP, MSWP [MPa]

Figure4

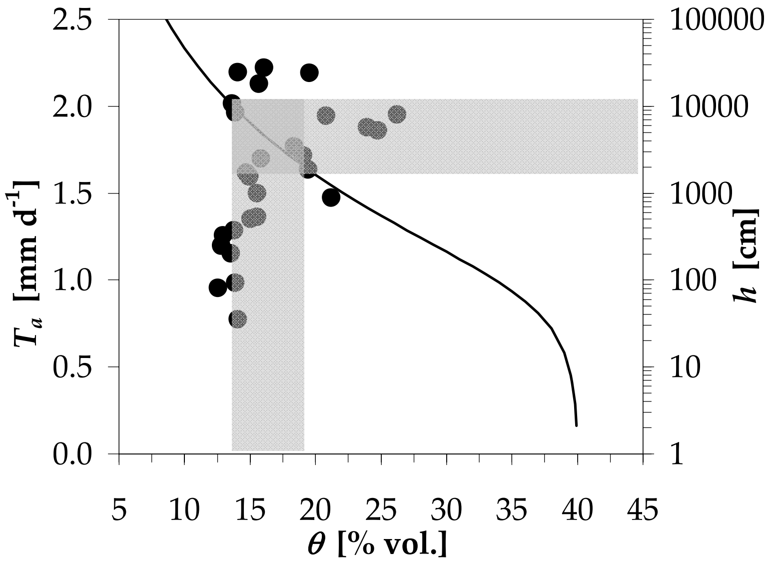

2.5
2.0
1.5
1.0
0.5
0.0
100000
10000
1000
100
10
1
T_a [mm d^{-1}]
h [cm]
5 10 15 20 25 30 35 40 45
θ [% vol.]

Figure5

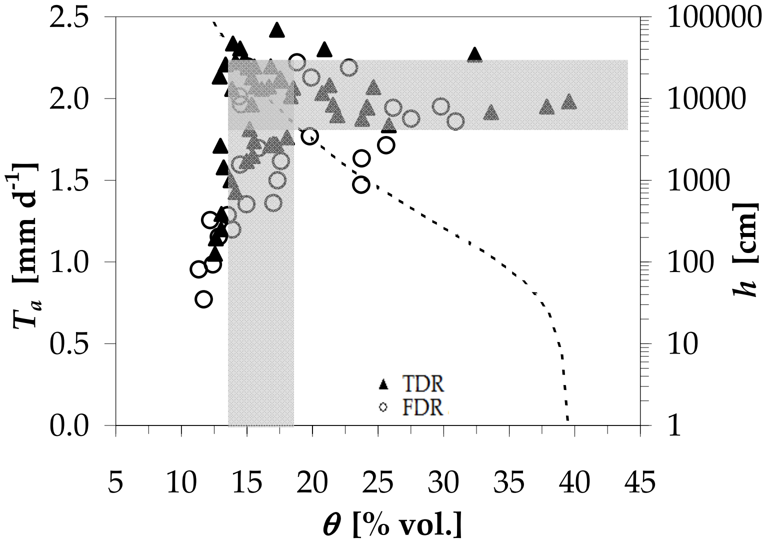

2.5
2.0
1.5
1.0
0.5
0.0
T_a [mm d^{-1}]
100000
10000
1000
100
10
1
h [cm]
5
10
15
20
25
30
35
40
45
θ [% vol.]
TDR
FDR

Figure6a

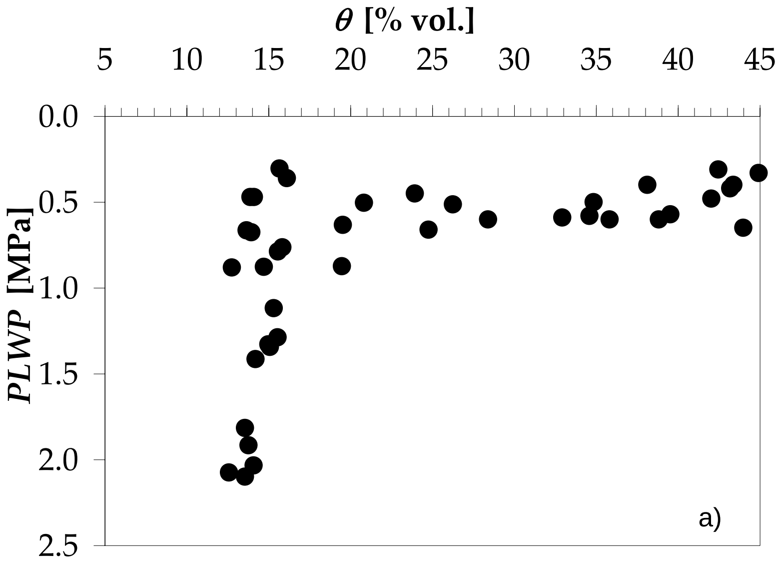

Figure6b

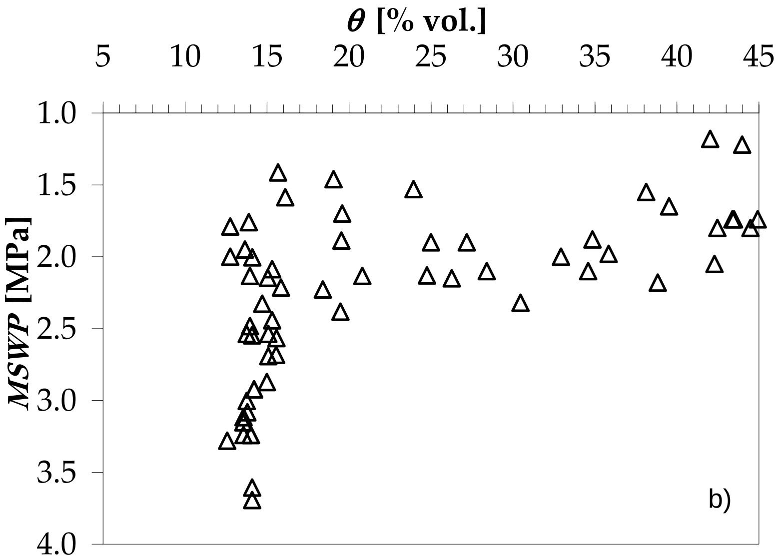

Figure6c

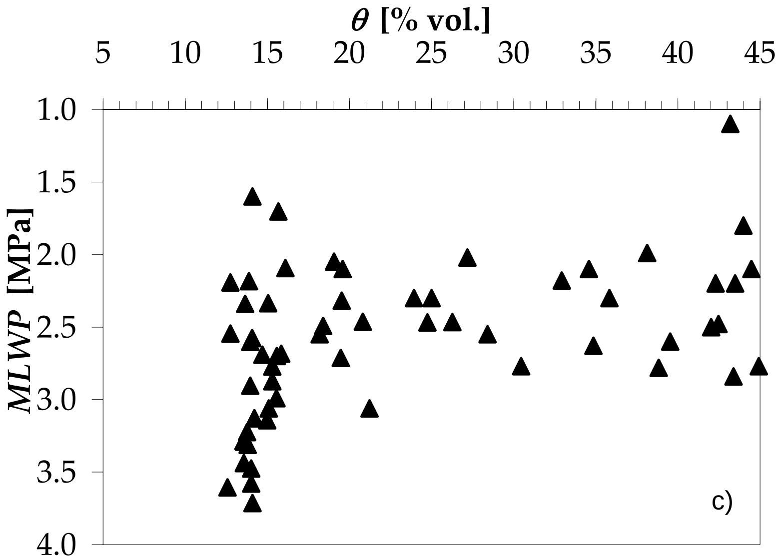

Figure7a

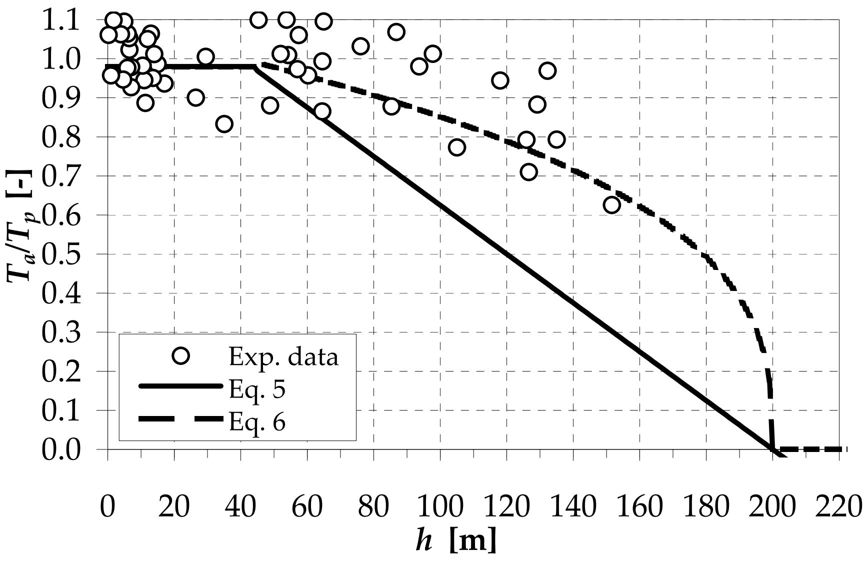

1.1
1.0
0.9
0.8
0.7
0.6
0.5
0.4
0.3
0.2
0.1
0.0
T_a/T_p [-]
Exp. data
Eq. 5
Eq. 6
0
20
40
60
80
100
120
140
160
180
200
220
h [m]

Figure7b

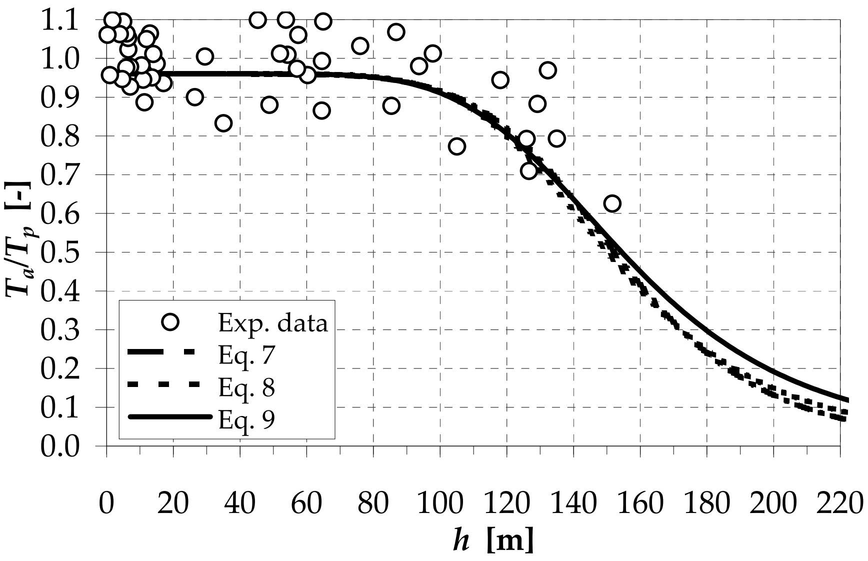
1.1
1.0
0.9
0.8
0.7
0.6
0.5
0.4
0.3
0.2
0.1
0.0
T_a/T_p [-]
Exp. data
Eq. 7
Eq. 8
Eq. 9
0
20
40
60
80
100
120
140
160
180
200
220
h [m]

Figure8a

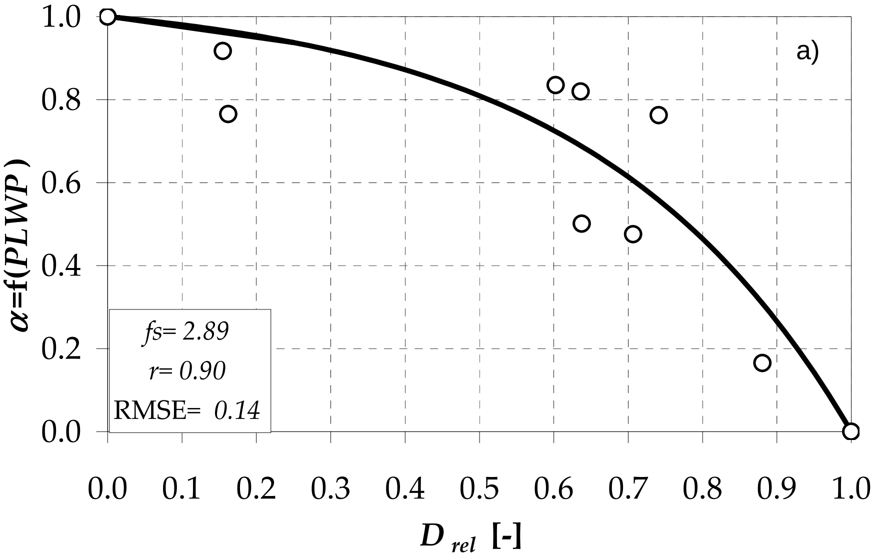

1.0
0.8
0.6
0.4
0.2
0.0
α=f(PLWP)
a)
fs= 2.89
r= 0.90
RMSE= 0.14
0.0 0.1 0.2 0.3 0.4 0.5 0.6 0.7 0.8 0.9 1.0
D rel [-]

Figure8b

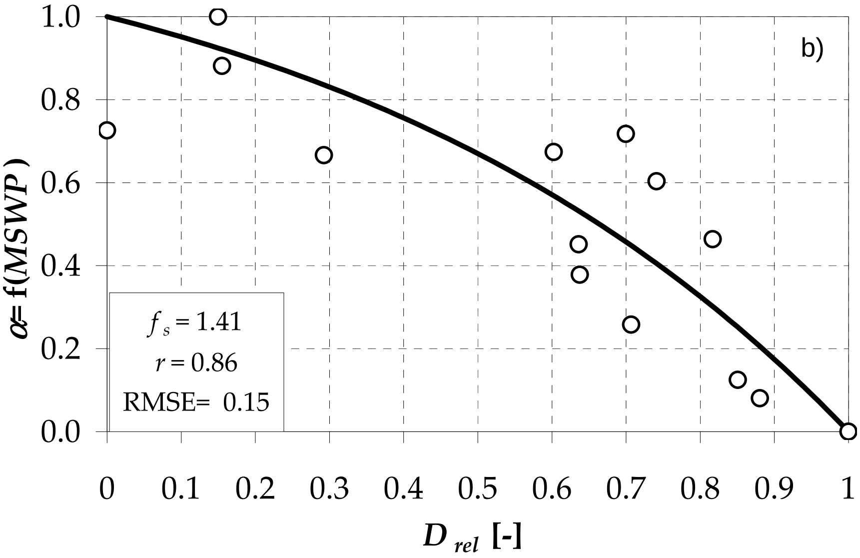

b)
f_s = 1.41
r = 0.86
RMSE= 0.15
1.0
0.8
0.6
0.4
0.2
0.0
α= f($MSWP$)
0
0.1
0.2
0.3
0.4
0.5
0.6
0.7
0.8
0.9
1
D_{rel} [-]

Figure Caption List

Fig. 1 – 2D maps of the Root Length Density distribution at different soil layers from 0 to 100 cm

Fig. 2 – Soil water retention curves for the four investigated layers and average curve for the entire soil profile. Soil water retention curves were determined on eight undisturbed soil samples, collected into soil volume where most of the root absorption takes place

Fig. 3 - Actual transpiration as a function of absolute values of predawn leaf water potential, *PLWP*, midday leaf water potential *MLWP* and midday stem water potential *MSWP*. Regression lines are also showed

Fig. 4 - Actual transpiration as a function of average soil water content in the layer 10-100 cm. The average water retention curve, for the same layer, is also represented. Shaded area indicates the range of variation of the observed critical soil water status

Fig. 5 - Actual transpiration as a function of average soil water content, in the layer 45-65 cm, measured with FDR (Frequency Domain Reflectometry) and TDR (Time Domain Reflectometry) techniques. Soil water retention curve in the same soil layer, is also showed. Shaded area indicates the range of variation of the observed critical soil water status

Fig. 6a-c –Experimental values of a) predawn leaf water potential, PLWP, b) midday leaf water potential MLWP c) midday stem water potential MSWP and corresponding soil water contents in the layer 10-100 cm

Fig. 7a, b – Experimental values of relative transpiration, T_a T_p^{-1}, as a function of soil matric potential, h, and fitted water stress models (eq. 5-9)

Fig. 8 a-b - Experimental values of the stress coefficient, α, as a function of relative depletion, D_{rel}, and fitted water stress model (eq. 10)

Tables

Click here to download Tables: TABLE.doc

Tab. 1

Depth [cm]	θ_s [cm^3 cm^{-3}]	θ_r [cm^3 cm^{-3}]	α [cm^{-1}]	n [-]	m [-]	ρ_b [Mg m^{-3}]
0	0.39	0.05	0.008	1.32	0.24	1.36
30	0.56	0.05	0.015	1.19	0.16	1.31
60	0.39	0.06	0.014	1.23	0.18	1.38
100	0.36	0.06	0.022	1.18	0.15	1.61
Average 10-100 cm	0.42	0.05	0.015	1.23	0.18	1.41
Average 45-65 cm	0.47	0.05	0.014	1.21	0.17	1.34

Tab. 2 –

DATA	Irrigation Depth [mm]	Rainfall Depth [mm]
12-Jul-08	30.6	
30-Jul-08		0.6
12-Aug-08	30.6	
13-Aug-08	30.6	
14-Aug-08	30.6	
26-Aug-08		12.6
Total 2008	**122.4**	**12.6**
13-Jul-09	5.1	
5-Aug-09	30.6	
6-Aug-09	30.6	
7-Aug-09	30.6	
19-Aug-09	17.8	
20-Aug-09	12.7	
21-Aug-09		5.2
26-Aug-09		5.2
Total 2009	**127.4**	**10.4**

Tab. 3 -

Variable	Value	
	Max	**Min**
Air Temperature [°C]	39.7	25.4
Air relative humidity [%]	69.0	16.0
Vapor pressure deficit [kPa]	5.4	1.2
Wind velocity at 10 m [m s^{-1}]	5.4	1.1
Wind velocity at 2 m [m s^{-1}]	3.3	0.7
Solar Radiation [W m^{-2}]	949.5	533.8
Net Solar Radiation [W m^{-2}]	720.7	408.5
Soil Water content [% vol.]	44.0	38.0
Predawn leaf water potential [MPa]	-0.36	-0.50
Canopy temperature [°C]	38.2	23.5

Tab. 4 -

Eq.	**Mathematical Formulation**	***h_3* or *h** [m]**	***h_4* or *h_{max}* [m]**	***h_{50}* [m]**	***α_0***	***a***	***p***	***r***
1	$\alpha(h) = \frac{h - h_4}{h_3 - h_4}$	40	200					0.63 (n.s.)
2	$\alpha(h) = \left(\frac{h - h_4}{h_3 - h_4}\right)^a$	40	200			0.34		0.64 (0.05)
3	$\alpha(h) = \frac{1}{1 + \left(\frac{h}{h_{50}}\right)^p}$			152			4.284	0.65 (0.05)
4	$\alpha(h) = \frac{1}{1 + \left[\frac{(h^* - h)}{(h^* - h_{50})}\right]^p}$	40		152			3.137	0.66 (0.05)
5	$\alpha(h) = \frac{1}{1 + \frac{(1 - \alpha_0)}{\alpha_0}\left[\frac{(h^* - h)}{(h^* - h_{max})}\right]^p}$	40	200		0.15		4.388	0.66 (0.05)

Tables caption list
Click here to download Tables: Table Caption List.doc

Table Caption List

Tab. 1 – van Genuchten parameters (θ_r, θ_s, α, n, m) and bulk density (ρ_b) for the 4 investigated soil layers. Parameters of the average water retention curves, determined at 10-100 and 45-65 cm, are also showed. θ_r= residual soil water content; θ_s= saturated soil water content; α, n, m: fitting parameters

Tab. 2 – Irrigation scheduling and rainfall depth in the period from July 1 to Aug 31, 2008 and 2009

Tab. 3 - Maximum and minimum hourly values of collected environmental variables for well watered trees, used to estimate the minimum canopy resistance

Tab. 4 - Critical thresholds of soil water status and parameters of the examined models. Pearson correlation coefficient, *r*, and statistical significance are also showed